# Full-dimensional, High-level ab initio Potential Energy Surfaces for $H_2(H_2O)$ and $H_2(H_2O)_2$ with Application to Hydrogen Clathrate Hydrates

Zahra Homayoon,[1, a)] Riccardo Conte,[1] Chen Qu,[1] and Joel M. Bowman[1, b)]

*Cherry L. Emerson Center for Scientific Computation and Department of Chemistry, Emory University, Atlanta, Georgia 30322, USA*

(Dated: 3 July 2015)

New full-dimensional potential energy surfaces, obtained upon precise least-squares fitting of high-level electronic energy databases, are reported for intrinsic $H_2(H_2O)$ two-body and $H_2(H_2O)_2$ three-body potentials. The database for $H_2(H_2O)$ consists of approximately 44,000 energies at the CCSD(T)-F12b/aug-cc-pVQZ level of theory, while the database for the three-body interaction consists of more than 36,000 energies at the CCSD(T)-F12a/haTZ (aug-cc-pVTZ for O, cc-pVTZ for H) level of theory. Two precise potentials are based on the invariant-polynomial technique, and are compared to computationally faster ones obtained via "purified" symmetrization. All fits use reduced permutational symmetry appropriate for these non-covalent interactions. These intrinsic potentials are employed together with existing ones for $H_2$, $H_2O$, and $(H_2O)_2$, to obtain full PESs for $H_2(H_2O)$ and $H_2(H_2O)_2$. Properties of these full PESs are presented, including a diffusion Monte Carlo calculation of the zero-point energy and wave function of the $H_2(H_2O)$ dimer. These PESs together with an existing one for water clusters are used in a many-body representation of the PES of hydrogen clathrate hydrates, illustrated for $H_2@(H_2O)_{20}$. An analysis of this hydrate is presented, including the the electronic dissociation energy to remove $H_2$ from the calculated equilibrium structure.

[a)]Current address: Department of Chemistry and Biochemistry, Texas Tech University

[b)]Electronic mail: jmbowma@emory.edu

## I. INTRODUCTION

Interactions of molecular species with $H_2O$ lead to the formation of van der Waals complexes of great importance for energy applications, and for research fields like astrochemistry and combustion chemistry. A relevant example, which has drawn considerable attention both theoretically and experimentally,[1–6] is provided by the $H_2{-}H_2O$ dimer, in which the water molecule exhibits an interesting dual identity as either proton donor or acceptor.

Detailed computational investigations of this dimer require an accurate representation of the potential energy surface (PES). An early PES of the $H_2{-}H_2O$ dimer has been reported by Hodges *et al.*[7] in 2004. This was a rigid-body, five-dimensional PES obtained with scaled perturbation theory. In 2005, Faure *et al.*[8] presented a full-dimensional interaction potential, calibrated using highly accurate and explicitly correlated wave functions at the CCSD(T)-R12 level of theory. They first calculated the $H_2{-}H_2O$ interaction by performing rigid-rotor five-dimensional calculations for a large number of geometries at "medium accuracy" CCSD(T) level. The resulting surface was further calibrated by means of high-precision explicitly correlated CCSD(T)-R12 calculations on a subset of the rigid-rotor intermolecular geometries. Finally, the five-dimensional rigid-rotor PES was extended to all nine dimensions. Later they reported a vibrationally averaged potential for the dimer.[9] This PES was then used to investigate rovibrational states of the $H_2{-}H_2O$ dimer, showing good agreement with experimental observations.[5] The extension beyond the rigid rotor was made using a quadratic Taylor series expansion about the rigid rotor reference configuration. It has not, to the best of our knowledge, been used for vibrational applications beyond zero-point averaging of the full potential.

The interaction between water molecules and other molecular species is also crucial in

clathrate hydrates, which are of widespread interest owing to their role in energy storage. Methane hydrates, for example, are a potential source of energy and also may be responsible for flow reduction in gas pipelines.[10] Another key example, and one focus of this paper, is the hydrogen clathrate hydrate, which is potentially an environmentally friendly and efficient material for hydrogen storage. These clathrate hydrates are characterized by a regularly ordered water skeleton, with $H_2O$ molecules forming hydrogen bonded cages, in the case of hydrogen hydrates, which have recently attracted much theoretical and experimental attention,[11–15] three main structures have been observed, consisting of cages of water molecules with a hydrogen molecule embedded inside. Two of them are cubic structures, called type I (sI), and type II (sII), while a third structure is a hexagonal one, named type H (sH). The cubic sI unit cell has 46 water molecules that form two pentagonal dodecahedron ($5^{12}$) and six hexagonal truncated trapezohedron ($5^{12}6^2$) cages. In the case of type sII, the cubic unit consists of 136 water molecules organized in sixteen $5^{12}$ and eight $5^{12}6^4$ cages. Finally, the unit cell for the sH hydrate is made of 34 water molecules, which form three different types of cages, namely $5^{12}$, $4^3 5^6 6^3$, and $5^{12}6^8$.[16]

As a potential material for hydrogen storage, the stability of hydrogen clathrate hydrates with respect to hydrogen occupancy has been studied theoretically. An early study of the thermodynamical stability of hydrogen hydrates has been performed by means of DFT and MP2 by Patchkovskii and Tse[17]. Later, structure and stability of hydrogen hydrates were investigated using density functional theory by Chattaraj, Bandaru, and Mondal[18]. They optimized four different cages, i.e. $5^{12}$, $5^{12}6^2$, $5^{12}6^4$, and $5^{12}6^8$, at the B3LYP/6-31G(d) level of theory and performed MP2/3-21G single point energy calculations on the DFT-optimized geometries. The occupancy of different cages in hydrogen clathrate hydrates has also been studied experimentally[14,15,19,20] and theoretically via thermodynamic model,[21],

molecular dynamics simulations,[22] Monte Carlo simulations,[23,24] and quantum translation-rotation calculations.[25–27] The possibility of hydrogen double occupancy in the dodecahedral cage has been explored experimentally.[15,28] The hydrogen migration in clathrates has also been studied.[29,30] In addition, previous theoretical studies have investigated the translation-rotation eigenstates and wavefunctions, mainly by employing rigid water cages and high-level $H_2-H_2O$ two-body potentials.[31–33] Recently these translation-rotation dynamics calculations have been compared with experimental inelastic neutron scattering spectra.[34,35]

For theoretical studies, clathrate hydrates are large and complex systems, where direct *ab initio* calculations can only employ relatively low levels of theory; a more demanding, high-level study of clathrate hydrates can be tackled by means of an analytical PES of the cluster constructed on the basis of a many-body representation approach. In this representation, interaction PESs are combined with high-level intramolecular surfaces of the isolated molecules, and the representation is truncated at a level sufficiently high to permit a reliable description of energetic, vibrational and dynamical properties of the cluster. In previous quantum studies, the interaction between $H_2$ and the water molecules was assumed to be pairwise additive, based on two different types of $H_2-H_2O$ pair potentials, such as a simple point charge model (SPC/E)[22], and the *ab initio* one by Hodges *et al.*[7]. However, quantum calculations using the five-dimensional *ab initio* PES overestimate the angular anisotropy of the $H_2-H_2O$ cage interaction, yielding too large $H_2$ rotational splittings, and underestimate the translational frequencies; on the contrary, the same calculations using SPC/E potential, which actually incorporates approximately some effect of nonadditive, many-body induced polarizations, yield better agreement with experiment.[34] This implies that three-body $H_2-H_2O-H_2O$ interactions cannot be neglected. Furthermore, the occupancy of cages are still under debate, so more demanding investigations of this problem certainly require

the inclusion of the three-body interactions.

The importance of $H_2$ hydrates and deviation of existing theoretical results from experimental data motivated us to construct a full-dimensional, high-level, global potential energy surface for $H_2(H_2O)_n$. Our PES is a many-body representation truncated at the three-body level. It adopts already available PESs for $H_2$, $H_2O$, $(H_2O)_2$, and $(H_2O)_3$ plus new, high-quality ones for the intrinsic $(H_2{-}H_2O)$ and $(H_2(H_2O)_2)$ interactions, reported here. Several fits for these intrinsic potentials are reported; these have different fitting precision and, especially for the $(H_2(H_2O)_2)$, different computational timings. Thus, depending on the application a different choice from the "menu" of fits can be made.

The paper is organized as follows. In the next section we provide details about the electronic calculations and the construction of the new intrinsic PESs. The PESs are tested by evaluating dimer and trimer energetics, one-dimensional cuts, and harmonic frequencies at relevant geometries. Then, diffusion Monte Carlo calculations of the $H_2{-}H_2O$ dimer zero-point energy and wave function are presented along with the dissociation energy $D_0$. Finally, we apply the many-body PES to one hydrogen molecule encapsulated in a $5^{12}$ water cage. Its optimized structure is reported and the contributions of two- and three-body interactions to its dissociation energy are evaluated. A Summary and Conclusions constitute the last section of the paper.

## II. THEORETICAL AND COMPUTATIONAL DETAILS

### A. *Ab initio* Calculations

For calculations of the intrinsic two-body $H_2{-}H_2O$ energies, the CCSD(T)-F12 method was employed, and tests of various basis sets were performed to evaluate their accuracy and

efficiency, in order to come up with a reasonable choice for the database of energies for fits. For this purpose the *ab initio* dissociation energy ($D_e$) of the $H_2-H_2O$ dimer was calculated at the CCSD(T)-F12b level of theory using aVTZ, aVQZ and aV5Z basis sets for the global and secondary minima. The results are given in Table I, along with the result from previous CCSD(T)-R12 calculations using theoretical equilibrium geometries.[8] Compared to the aV5Z result, $D_e$ calculated using aVTZ is about 20 $cm^{-1}$ larger, while overestimation by aVQZ is only 5 $cm^{-1}$. Therefore, the aVQZ basis seems to be a reasonable choice for accuracy, and the estimated computational cost of the calculations for the database of roughly nine days of CPU time on a sixteen-processor computer, was deemed quite feasible.

TABLE I. Comparison of $D_e$ (in $cm^{-1}$) for $H_2-H_2O$ dimer using different basis sets and from a previous study.

| Minimum Geometry | aVTZ | aVQZ | aV5Z | Ref. 8 |
|---|---|---|---|---|
| Global | 242.2 | 228.9 | 224.2 | 221.2 |
| Secondary | 222.0 | 204.3 | 198.9 | - |

Thus, for the two-body intrinsic potential we generated a database of 44,623 *ab initio* energies at CCSD(T)-F12b level of theory with aVQZ basis set. A first set of $H_2-H_2O$ configurations was obtained by means of direct-dynamics simulations performed upon normal-mode sampling at several internal excitation energies up to the dissociation limit and employing B3LYP/6-31G(d,p) level of theory. Then, starting from many of the distorted monomer configurations thus generated, additional dimer geometries were randomly sampled by varying inter-monomer H-O or H-H distances in the range between 2.0 and 9.0 Angstroms. At these configurations, the intrinsic two-body interaction ($V_{2b}^{H_2-H_2O}$) was obtained according

to

$$V_{2b}^{H_2-H_2O} = V^{H_2-H_2O} - V^{H_2} - V^{H_2O}. \quad (1)$$

Thus, three electronic energies are needed per configuration. From the database of these energies, a preliminary two-body fit was performed to assess the appropriateness of the sampled configurations. Harmonic frequencies of the global minimum and some one-dimensional cuts obtained with this preliminary PES were compared to the corresponding values from *ab initio* calculations. Thereby, about 3,000 points were added to the preliminary dataset to provide a better coverage of the surface.

For the three-body intrinsic $H_2-H_2O-H_2O$ potential, we employed a CCSD(T)-F12a level of theory and haTZ (aVTZ for O and VTZ for H) basis set. The database consists of 36,603 *ab initio* energies. A first set of 29,757 points was generated following the same procedure adopted for the two-body database as described above. The remaining 6,846 points were selected from clathrate structures. The intrinsic $H_2-H_2O-H_2O$ three-body energy has been calculated on the basis of

$$V_{3b}^{H_2(H_2O)_2} = V^{H_2(H_2O)_2} - V_{2b}^{(H_2O)_2} - \sum_{i=1}^{2} V_{2b}^{H_2-H_2O(i)} - \sum_{i=1}^{2} V^{H_2O(i)} - V^{H_2}. \quad (2)$$

All the *ab initio* calculations were carried out using MOLPRO 2010 software.[36]

## B. PES Fitting

To fit the intrinsic potentials, two different fitting techniques have been employed. Both of them lead to the generation of fitting bases made of polynomials that are invariant with respect to translation, rotation and permutations of like atoms as specified by the permutational group given as an input. For the $H_2-H_2O$ two-body potential, the permutational group we have adopted is labelled, using notation we introduced previously,[37,38] as 221, mean-

ing that in this five-atom system the two (2) hydrogens of $H_2$ can be interchanged without modification of the potential energy. The same applies to the two (2) hydrogens of the $H_2O$ monomer, while the single oxygen atom (1) does not have a permutational counterpart. In the case of the $H_2{-}H_2O{-}H_2O$ three-body potential, an eight-atom system, the potential energy must also be invariant for monomer exchange (i.e. the two water monomers can be listed in any of the two possible relative orders). If this additional symmetry is not already included in the permutational group, it may be incorporated by duplicating the database of *ab initio* energies, similarly to what we have done in a previous study of $CH_4{-}H_2O{-}H_2O$.[38] In this circumstance, we append the $^*$ symbol to the permutational group label. For the three-body potentials, we have employed either symmetry $22211^*$ or symmetry 422, which does include monomer-exchange invariance because the four (4) water hydrogens and two (2) water oxygens are allowed to permute (as well as the two (2) $H_2$ hydrogens). Reduced permutational symmetry has been shown to be adequate for systems, like the one here presented, where interactions are non-covalent and there is no exchange of atoms between different monomers.[37,38] Reduced permutational symmetry has also been used to represent the water dimer and trimer potentials in symmetrized monomials (see below).[39]

One fitting technique we have used is based on the efficient invariant-polynomial decomposition.[40] In this case, the polynomial fitting basis is made of factored polynomials. Specifically,

$$V(\boldsymbol{y}) = \sum_{d=0}^{M} C_{ab} h_a[p(\boldsymbol{y})] q_b(\boldsymbol{y}). \tag{3}$$

$p(\boldsymbol{y})$ are called primary invariant polynomials. Their number equals the number of internuclear distances in the system (10 for the intrinsic two-body potential, and 28 for the intrinsic three-body surface). $h_a$ is a polynomial of the primary invariants, while $q_b$ indicates a secondary invariant polynomial. In Eq. (3), $d$ is the total polynomial order, i.e. the sum of the orders of $h_a$ and $q_b$. Its maximum value is set to $M$. A linear coefficient $C_{ab}$ is associated to

each polynomial in the fitting basis and determined upon fitting of the available database of *ab initio* energies. Primary and secondary invariants depend on Morse variables defined as $y_{ij} = \exp\{-r_{ij}/\lambda\}$, where $r_{ij}$ is the internuclear distance between atoms $i$ and $j$, and $\lambda$ is a parameter usually in the range between 2 and 3 au. In the present work, we have assigned to $\lambda$ a value equal to 2 au. The fitting basis obtained by means of Eq. (3), which we label with letter F (for "Full"), provides a very precise potential, but contains some terms that return a small non-zero contribution when monomers are separated.

The second fitting technique employed is based on monomial symmetrization.[40,41] It usually provides a slightly less precise fit, but the basic technique can be modified to incorporate rigorously the zero-interaction asymptotic limit of intrinsic many-body interactions.[38,42] A similar extension for the primary and secondary invariant approach is currently in progress. Specifically, given the permutational group and the maximum polynomial order as input, the monomial symmetrization technique[41] is based on the following expression for the potential energy

$$V(\boldsymbol{y}) = \sum_{m=0}^{M} D_{\underline{l}}\, \mathcal{S}\left[\prod_{i<j}^{N_{at}} y_{ij}^{l_{ij}}\right] \quad (m = \sum l_{ij}), \tag{4}$$

where $y_{ij}$ are the same Morse variables defined above. $D_{\underline{l}}$ are linear coefficients, determined by means of a least-squares fit, and $\underline{l}$ stands for the ordered collection of exponents of the Morse variables ($l_{ij}$). $N_{at}$ is the number of atoms in the system. Again, we set the $\lambda$ parameter of the Morse variables equal to 2 au. $\mathcal{S}$ is the formal operator that symmetrizes the monomials according to the chosen permutational group.

The basic scheme provided by Eq. (4) has been modified by discarding those polynomials which returns a non-zero value when one (or more) of the monomers is set a far distance away from the others. Hereafter, we identify these potentials with the letter P, which stands

for "Purified". The purified basis can be further reduced by keeping only those polynomials that depend exclusively on inter-monomer distances. We label the final fitting basis (and potential) as PP, which stands for "Pruned Purified". PP potentials feature a consistent reduction of computational costs, usually at the price of moderately reduced accuracy. More details about the computational procedures for purification and pruned purification can be found in Ref. 38.

### C. Diffusion Monte Carlo

Diffusion Monte Carlo (DMC) is a powerful method to determine the exact zero-point wavefunction and energy of a system.[43] It solves in a statistical way the time-dependent Schrödinger equation in imaginary time ($\tau$). The simple unbiased algorithm was applied in this work.[44,45] In brief, an ensemble of walkers represents the configurations of the molecule. These walkers are propagated via "birth-death" process.[46] After each step, the reference energy, $E_{ref}(\tau)$, is calculated as $E_{ref}(\tau) = \langle V(\tau)\rangle - \alpha\left[N(\tau) - N(0)\right]/N(0)$, where $\langle V(\tau)\rangle$ is the average potential at time $\tau$ over all the walkers; $N(\tau)$ is the number of walkers at time $\tau$, and $\alpha$ is a "feedback" parameter that controls the fluctuations of the number of walkers and the reference energy. In this study we chose $\alpha = 0.1$ a.u. Finally, the average of the reference energy over the imaginary-time gives an estimate of the zero-point energy. For each system studied, ten simulations were carried out, and in each simulation, 20,000 walkers were propagated for 55,000 steps with step size, $\Delta\tau$, of 5.0 a.u. The system was equilibrated for the first 5,000 steps and then the reference energy was collected and averaged. It is perhaps worth noting that this method does require a global or semi-global PES, as of the order of $10^9$ potential evaluations are needed per simulation.

## III. RESULTS AND DISCUSSION

We have obtained several fits for the intrinsic $H_2-H_2O$ and $H_2-H_2O-H_2O$ interactions, adopting the techniques described in the previous section. The potentials have been first assessed on the basis of their fitting root mean square error (rmse) and relative computational costs. Table II summarizes these for each potential, identified by the label of the corresponding fitting basis (F-, P-, PP-), as described in the previous Section, followed by the permutational group / maximum polynomial order employed. The computational times are evaluated by averaging batches of 10 series of 50,000 potential calls, and compared by setting arbitrarily to 100 the cost of F-221/6 (i.e. the potential obtained for the two-body interaction by means of the fitting technique based on the invariant polynomial decomposition).

Table II shows that for the two-body interaction F-221/6 is characterized by a very small fitting error. The purified potential (P-221/6) still has low rmse and speeds up calculations by a factor of two. The pruned purified potential (PP-221/6) depends on a much smaller number of coefficients and it is extremely fast but, on the other hand, its fitting rmse is much higher. This can be explained by recalling that PP potentials are based exclusively on inter-monomer variables. In the two-body system here presented there are only six inter-monomer distances, which is fewer than the dimensionality of the $H_2-H_2O$ surface (nine). Finally, we notice that an increment of the maximum polynomial order (P-221/7) decreases only slightly the fitting error but increases about three times computational overheads. For these reasons, we will employ F-221/6 and P-221/6 in our further calculations.

Moving to the three-body potentials, we first notice that the potential obtained by means of the invariant polynomial technique (F-422/5) is very accurate but also very slow, and the

TABLE II. Number of coefficients, fitting root mean square error, and relative computational times, for different fitted $H_2-H_2O$ (upper) and $H_2-H_2O-H_2O$ (bottom) intrinsic potentials. The type of polynomial basis is full (F), purified (P), or pruned purified (PP). Time is arbitrarily set equal to 100 for F-221/6.

| $H_2-H_2O$ | No. Coeff. | rmse ($cm^{-1}$) | time (arb. units) |
|---|---|---|---|
| F-221/6 | 2,304 | 3.8 | 100 |
| P-221/6 | 2,174 | 5.0 | 53 |
| PP-221/6 | 260 | 114.8 | 7 |
| P-221/7 | 5,216 | 4.2 | 153 |
| $H_2-H_2O-H_2O$ | No. Coeff. | rmse ($cm^{-1}$) | time (arb. units) |
| F-422/5 | 5,801 | 2.9 | 2,378 |
| P-422/5 | 2,850 | 9.4 | 1,128 |
| PP-22211*/5 | 9,649 | 6.5 | 390 |
| P-22211*/4 | 4,455 | 12.7 | 186 |

purified potential for the same permutational group (P-422/5) cut costs just in half. Better results are obtained lowering the order of the permutational group. The potentials for group 22211* are faster to evaluate even if they depend on a larger number of coefficients (and consequently polynomials). The reason is that the single polynomials are much cheaper to calculate than in the case of symmetry 422. Accuracy for PP-22211*/5 and P-22211*/4 is also very good. In the case of the three-body interaction, the pruned purified potential depends on 21 inter-monomer variables, a number larger than the dimensionality of the $H_2-H_2O-H_2O$ surface (18), and the fitting rmse remains small. Due to their combined

accuracy and speed, PP-22211*/5 and P-22211*/4 will be employed in the trimer calculations together with F-422/5. Finally, we note, that computational times for the three-body fits are much larger than for the two-body fits, as expected.

A more detailed examination of the fitting precision and other properties is given next for the $H_2-H_2O$ and $H_2-H_2O-H_2O$ surfaces.

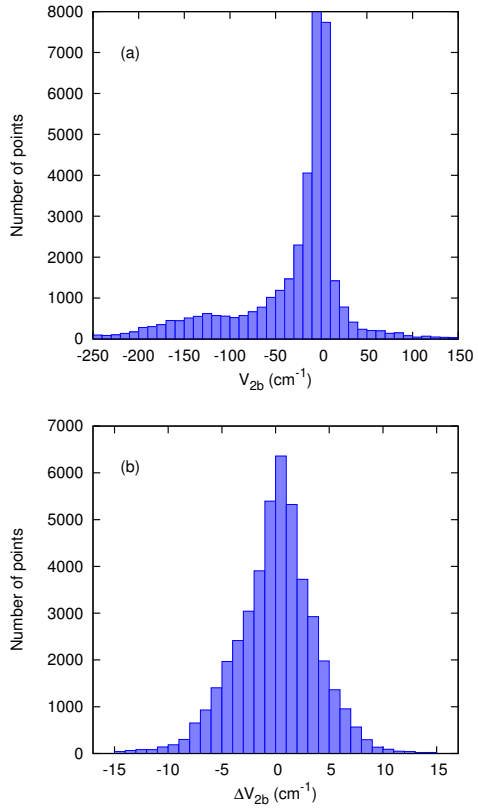


FIG. 1. Distribution of (a) energy and (b) fitting error (full fitting basis) of intrinsic two-body energies.

## A. Two-body potential and its application to the $H_2-H_2O$ dimer

Figure 1 shows the distribution of the intrinsic two-body energy and the corresponding fitting error when using the full fitting basis. The interaction between $H_2$ and water is fairly

small, with most of the sampled energies between -250 and 150 $cm^{-1}$. A large number of points were sampled at large monomer separation so that the F-potential is forced to be zero in the asymptotic region. These points contribute to the high peak at $V_{2b} = 0$ in the upper panel. The lower panel shows the distribution of the fitting error, which, in general, is lower than 15 $cm^{-1}$, with rmse of 3.8 $cm^{-1}$.

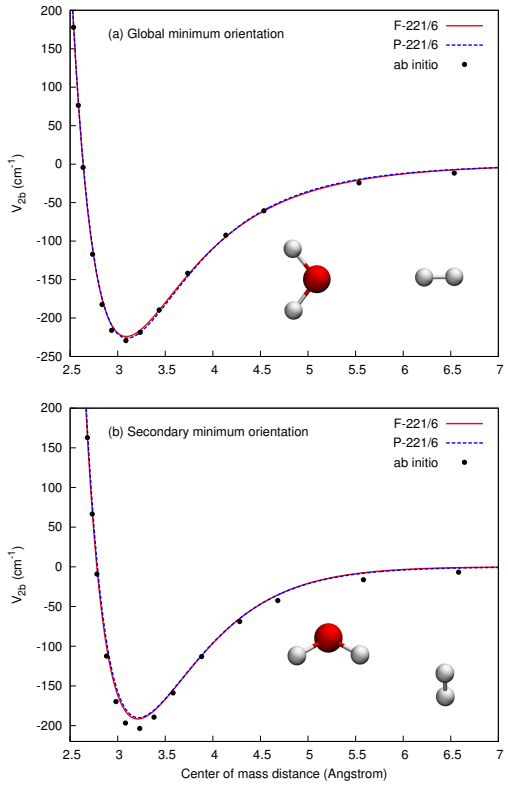


FIG. 2. Two one-dimensional cuts from the two-body PESs and *ab initio* calculations, at two different orientations.

Two one-dimensional cuts at two different orientations of the $H_2$−$H_2O$ dimer from *ab initio* calculations and the PES are given in Figure 2, which shows very good agreement between the F-221/6 and P-221/6 fits. Both fits slightly underestimate the well-depth in the second cut, but generally the agreement between the fits and the *ab initio* results is very good.

The global full PES of the $H_2-H_2O$ dimer is the sum of the intrinsic two-body potential (here either F-221/6 or P-221/6) and two pre-existing hydrogen and water monomer potentials.[47,48] This global $H_2-H_2O$ PES was employed for geometry optimization, calculation of the dissociation energy, normal mode analysis and DMC calculations of the zero-point energy and wavefunction of the dimer.

The two minima were located on the full PESs, and their configurations are depicted in panels (a) and (b) of Figure 3. The dissociation energies of these two minima are given in Table III. The dissociation energy of the global minimum agrees well with the *ab initio* value. The dissociation energy of the secondary minimum is underestimated by both PESs, but the difference from the *ab initio* values is within 15 $cm^{-1}$. The PES values are actually closer to the higher level *ab initio* ones, given in Table I. It should be noted that the monomer components of the full PES are of higher accuracy than the intrinsic two-body component, and so the apparent higher accuracy of the full PES may not be totally fortuitous.

TABLE III. $D_e$ (in $cm^{-1}$) for the $H_2-H_2O$ dimer from *ab initio* CCSD(T)-F12b/aVQZ calculations and two different PESs.

| Structure | *ab initio* | F-221/6 | P-221/6 |
|---|---|---|---|
| Global minimum | 228.9 | 223.7 | 225.8 |
| Secondary minimum | 204.3 | 191.4 | 189.8 |

The harmonic frequencies of the two minima are reported in Table IV. The *ab initio* frequencies for the first two modes are not shown because it's computationally too demanding to get well-converged frequencies for those low-frequency librations. Results for the two PESs agree well with each other. The agreement with the *ab initio* frequencies is also very good. Note also the small differences between the sets of frequencies for the intramolecular modes

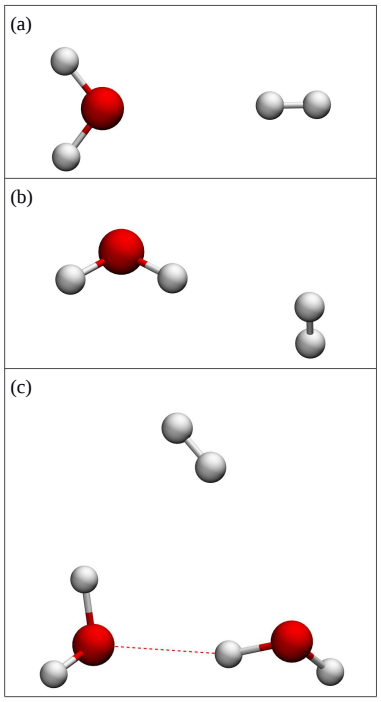


FIG. 3. The structures of (a) global minimum of $H_2{-}H_2O$ dimer, (b) secondary minimum of $H_2{-}H_2O$ and (c) global minimum of $H_2{-}H_2O{-}H_2O$ trimer.

of each minimum as well as the small shifts relative the isolated monomer frequencies (not shown). This is already an indication that these minima are actually quite "floppy". This is investigated in detail next.

The zero-point energies (ZPEs) of the dimer and the fragments have been calculated using DMC simulations. The ZPE of the bound dimer is $7003.8 \pm 1.2$ cm$^{-1}$ when employing F-221/6. If P-221/6 is used, then the ZPE is $7005.3 \pm 0.7$ cm$^{-1}$, which agrees very well with the F-221/6 result. The sum of ZPEs of the two fragments were calculated with two different approaches. The first approach still consists of DMC simulations but uses only the monomer PESs. The result is $6814.3 \pm 1.0$ cm$^{-1}$. In the second approach, the $H_2$ ZPE was calculated with a one-dimensional discrete variable representation (DVR), while the ZPE of water was calculated using the software MULTIMODE,[49] which solves the vibrational

TABLE IV. Harmonic frequencies of the two minima from *ab initio* and PES calculations.

| Global minimum | | | Secondary minimum | | |
|---|---|---|---|---|---|
| *ab initio* | F-221/6 | P-221/6 | *ab initio* | F-221/6 | P-221/6 |
| - | 33.1 | 36.9 | - | 39.3 | 39.4 |
| - | 34.9 | 38.3 | - | 82.7 | 85.4 |
| 144.9 | 132.8 | 132.8 | 117.3 | 100.7 | 101.1 |
| 265.6 | 259.0 | 262.3 | 146.4 | 135.8 | 133.9 |
| 295.2 | 281.4 | 281.2 | 358.2 | 337.3 | 330.8 |
| 1649.4 | 1649.4 | 1650.0 | 1650.3 | 1651.0 | 1651.1 |
| 3836.5 | 3831.0 | 3831.6 | 3836.4 | 3832.4 | 3834.9 |
| 3946.9 | 3943.0 | 3943.5 | 3945.5 | 3943.2 | 3943.0 |
| 4380.7 | 4380.6 | 4379.7 | 4387.8 | 4387.6 | 4387.9 |

Schrödinger equation rigorously, employing vibrational self-consistent field and virtual state configuration interaction methods. The sum of the two ZPEs of the fragments is in this case 6816.2 $cm^{-1}$, in agreement with the value obtained with DMC calculations. Finally, we evaluated the measurable dissociation energy ($D_0$) of the $H_2-H_2O$ dimer, and our best estimate is 187.6±1.2 $cm^{-1}$.

The vibrational ground state wavefunction of the dimer can also be obtained from the DMC simulation. About 2,000,000 geometries of the walkers were collected from the DMC simulations and these geometries were optimally aligned into the principal axis frame. The wavefunction amplitude was obtained by dividing the space into volume elements and performing histogram binning in the atomic coordinates. The vibrational ground state wavefunction of the $H_2-H_2O$ dimer is shown as cloud-like iso-surfaces in Figure 4, with two

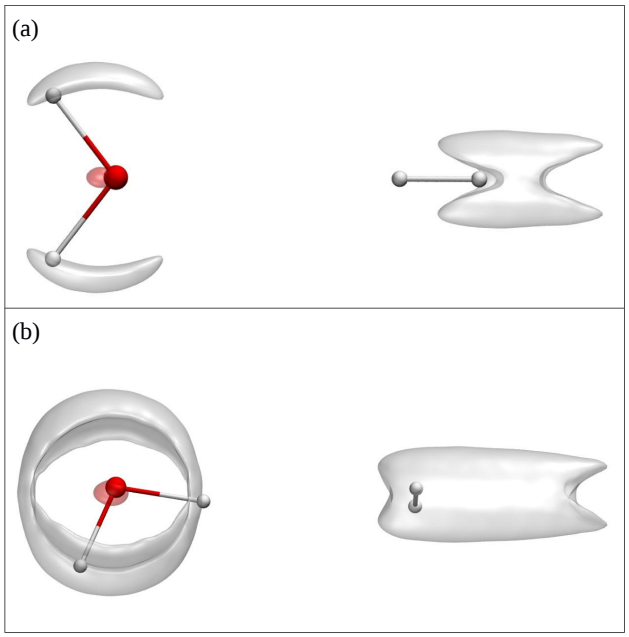


FIG. 4. Iso-surfaces of the vibrational ground state wavefunction for the $H_2-H_2O$ dimer from the DMC simulations with two different iso-values. The global and secondary structures are also indicated as reference structures in panels (a) and (b), respectively. See text for more details.

different iso-values. In the upper panel, the iso-value is 70.7% of the maximal amplitude, while, in the lower panel, the iso-value is 45% of the maximum. As a reference, the geometries of the global and secondary minima of the $H_2-H_2O$ dimer are also shown. As one can see from the figure, the wavefunction has larger amplitude near the global minimum, but also has significant amplitude near the secondary minimum. We conclude that, overall, the vibrational ground state wavefunction is broad and spans both minima, indicating that the dimer is characterized by large amplitude motion (i.e. nearly free monomer rotation).

### B. Three-body potential and its application to the $H_2-H_2O-H_2O$ trimer

Similar to the two-body case, Figure 5 shows the distribution of energy and fitting error for the F-422/5 intrinsic three-body potential. The intrinsic three-body energy is weaker

than the two-body one, and consequently the distribution of the energy is narrower. We also needed a large number of points at large monomer separation to guarantee zero asymptotic value in the case of the full fitting basis. Rmse (2.9 $cm^{-1}$) and fitting error distribution are comparable to those of the intrinsic two-body.

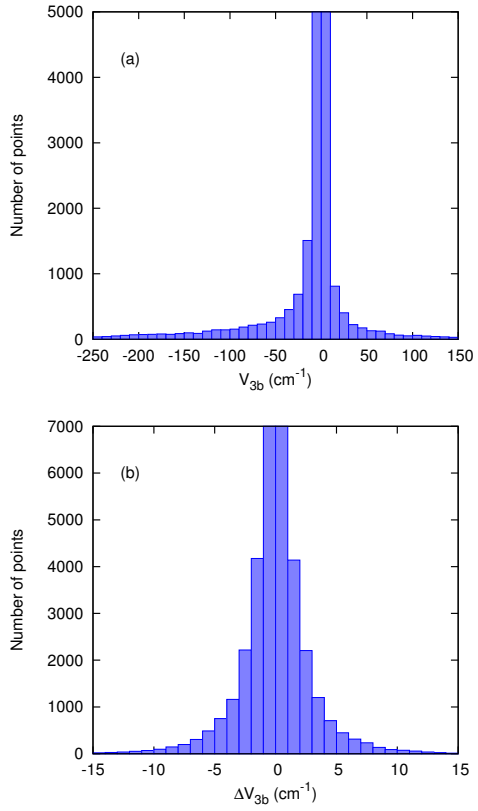


FIG. 5. Distribution of (a) energy and (b) fitting error (F-422/5 potential) of intrinsic $H_2-H_2O-H_2O$ three-body energies.

Two one-dimensional cuts that are not included in the fitting database are shown in Figure 6. Three fits of the three-body energy have been tested here. In one of the cuts, the fitted intrinsic potentials agree almost perfectly with the *ab initio* energies, while, in the other cut, the agreement is not perfect for F-422/5. It approaches zero slightly too fast when the O-O distance increases. However, overall, the fitted three-body potentials are precise

representations of the *ab initio* energies.

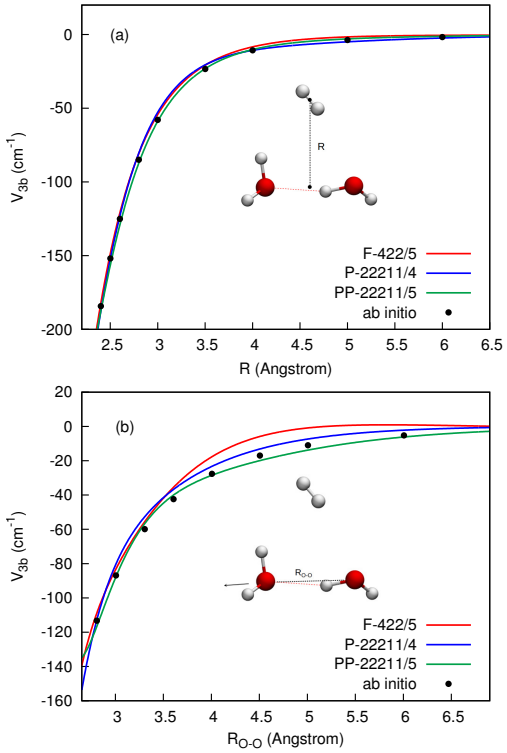


FIG. 6. Two one-dimensional cuts of the three-body interaction for the $H_2(H_2O)_2$ trimer from *ab initio* calculations and the indicated intrinsic three-body PESs.

The full, global PES of the $H_2{-}H_2O{-}H_2O$ trimer is the sum of five potentials: water monomer, $H_2$ monomer, $H_2{-}H_2O$ intrinsic two-body (F-221/6), previous water two-body from our group,[50] and $H_2{-}H_2O{-}H_2O$ intrinsic three-body. For the latter, three potentials were tested and compared, i.e. F-422/5, P-22211*/4 and PP-22211*/5. The structure of the trimer minimum is depicted in panel (c) of Figure 3. The electronic dissociation energy of the trimer, $D_e$, was determined by setting the zero of energy for the three isolated monomers in correspondence of their equilibrium geometry. The contribution of all the one-body, two-body and three-body terms as well as the final $D_e$ are listed in Table V. Note, the minima all differ slightly for each column in the table and so the contributions from all one-body and two-body terms differ slightly among the PESs, even though the same one-body and

two-body potentials are used in all PESs. The three analytical PESs all have somewhat smaller values of $D_e$ compared to the *ab initio* value. The difference is mainly due to the $(H_2O)_2$ two-body energy. The reason is that different *ab initio* methods were employed in the calculations. The potential we use for the water two-body in our analytical PESs has a near-exact $D_e$,[50] and thus more accurate than the one obtained with the present ab initio calculations, which use CCSD(T)-F12a/haTZ level of theory without counterpoise correction. Thus, we believe that accurate $D_e$ is within a few wavenumbers of 2140 $cm^{-1}$.

TABLE V. Energy of each term in the many-body decomposition of the $H_2(H_2O)_2$ trimer.

| | *ab initio* | F-422/5 | PP-22211*/5 | P-22211*/4 |
|---|---|---|---|---|
| $H_2$ one-body | 1.7 | 1.4 | 1.5 | 1.4 |
| $H_2O$ one-body | 15.6 | 13.7 | 14.0 | 13.7 |
| $H_2-H_2O$ two-body | -356.6 | -354.4 | -358.2 | -351.3 |
| $(H_2O)_2$ two-body | -1745.0 | -1703.3 | -1690.9 | -1703.4 |
| $H_2-(H_2O)_2$ three-body | -103.0 | -95.9 | -113.3 | -100.5 |
| $D_e$ | 2187.3 | 2138.5 | 2146.9 | 2140.1 |

Table VI gives the harmonic frequencies for the $H_2-H_2O-H_2O$ trimer. All the three PESs reproduce the frequencies accurately. However, if we just include the two-body interaction and neglect the $H_2-H_2O-H_2O$ interaction, the frequency of the $H_2$ stretch (the last row in the table) is overestimated. Overall the effects of the three-body interaction on the frequencies is small but not negligible. This is another confirmation that the $H_2-H_2O-H_2O$ intrinsic three-body contribution is notable and should not be neglected in both energetics calculations and harmonic-frequency analysis.

TABLE VI. Harmonic frequencies of intramolecular modes of the $H_2-H_2O-H_2O$ trimer from *ab initio* calculations and two different analytical potentials. Frequencies obtained neglecting the intrinsic three-body potential are listed in the last column.

| *ab initio* | F-422/5 | PP-22211*/5 | P-22211*/4 | Without three-body |
|---|---|---|---|---|
| 1648 | 1650 | 1651 | 1651 | 1650 |
| 1666 | 1666 | 1665 | 1664 | 1664 |
| 3740 | 3746 | 3748 | 3746 | 3754 |
| 3821 | 3823 | 3823 | 3822 | 3825 |
| 3914 | 3916 | 3916 | 3915 | 3916 |
| 3928 | 3931 | 3931 | 3932 | 3933 |
| 4355 | 4358 | 4356 | 4360 | 4372 |

### C. Application to the clathrate hydrates: $H_2$ in a $(H_2O)_{20}$ cage

It is now possible to assemble an analytical many-body potential energy surface for a general $H_2(H_2O)_n$ system, truncated at the three-body level. For this purpose, we need in addition to the potentials for the full $H_2-H_2O-H_2O$ the water three-body potential. We use the one contained in the general WHBB potential[50] (which includes potentials for water monomer, intrinsic two-body and intrinsic three-body). Given the fact that four and higher-body interactions for water clusters account for only a few percent (at most) of the total binding energies, neglecting those for hydrate clathrates is justified. We applied this analytical PES to optimize the geometry of a hydrogen molecule in a water $5^{12}$ cage. For the application shown here, we used our "F" potentials for both $H_2-H_2O$ and $H_2-H_2O-H_2O$ interactions. The optimized geometry of $H_2@(H_2O)_{20}$ on the many-body PES is shown in

Figure 7.

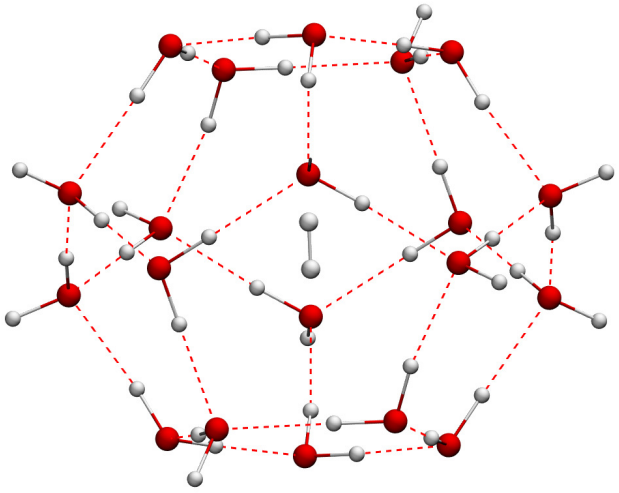

FIG. 7. The optimized geometry of one $H_2$ molecule in a $5^{12}$ $(H_2O)_{20}$ cage.

To assess the accuracy of our potentials in clathrate applications, we evaluated the dissociation energy of the $H_2@(H_2O)_{20}$ cluster, calculated as $D_e = E_{H_2} + E_{cage} - E_{H_2@(H_2O)_{20}}$, where $E_{H_2}$ and $E_{cage}$ are respectively the energies of the isolated $H_2$ and the empty cage (at their equilibrium geometry), while $E_{H_2@(H_2O)_{20}}$ is the energy of the optimized $H_2@(H_2O)_{20}$ cluster. In addition, the contributions of the 20 $H_2-H_2O$ two-body interactions and the 190 $H_2-H_2O-H_2O$ terms in the cluster were also evaluated. These two-body and three-body contributions were also estimated via *ab initio* CCSD(T)-F12a/haTZ calculations on the PES-optimized cluster geometry. The results are given in Table VII. For the two-body, the difference between *ab initio* and PES values is only 0.26 kcal/mol, and this can be due to the different levels of electronic structure theory employed. The *ab initio* calculations were based on CCSD(T)-F12a/haTZ, while the PES employed CCSD(T)-F12b/aVQZ. The many three-body interactions are small and of opposite signs in this cluster, but still contribute 0.14 kcal/mol to the $D_e$. Finally, the PES predicts that the dissociation energy, $D_e$, of $H_2@(H_2O)_{20}$ is 2.67 kcal/mol. This value is about 1 kcal/mol larger than the value

predicted by a MP2/6-31G(d) calculation (see Table VII).[18]

TABLE VII. The dissociation energy (in kcal/mol) of $H_2@(H_2O)_{20}$ and the contributions of the $H_2-H_2O$ two-body and $H_2-H_2O-H_2O$ three-body interactions.

| | *ab initio* | PES | MP2/6-31G(d) [a] |
|---|---|---|---|
| $D_e$ | - | 2.67 | 1.68 |
| $H_2-H_2O$ two-body | -2.29 | -2.55 | - |
| $H_2-(H_2O)_2$ three-body | -0.22 | -0.14 | - |

[a] Ref. 18

## IV. SUMMARY AND CONCLUSIONS

We have presented full-dimensional intrinsic two-body and three-body PESs of different accuracy and complexity for the $H_2-H_2O$ and $H_2-H_2O-H_2O$ interactions. The most accurate analytical PESs (F-221/6 for two-body and F-422/5 for three-body) have rmse of 3.8 and 2.9 $cm^{-1}$ respectively. They are obtained upon least-squares fits based on primary and secondary invariant polynomials with respect to permutations of like atoms. The other PESs are based on the symmetrized monomial approach and employ purified sets of polynomials as fitting bases. These purified PESs are not only computationally very efficient, but also able to ensure the correct zero-interaction asymptotic limit at large intermolecular distance, at the cost of just slightly lower accuracy.

The intrinsic potentials have been used to build a many-body PES for the general $H_2(H_2O)_n$ system. The accuracy of the PES has been assessed by applying it to the n=1 and n=2 cases, i.e. the $H_2-H_2O$ dimer and $H_2-H_2O-H_2O$ trimer. For the dimer, the PES can reproduce the *ab initio* electronic dissociation energy and the harmonic frequencies of

the dimer precisely. Our best estimation of the measurable dissociation energy ($D_0$) for the dimer is 187.6±1.2 $cm^{-1}$, based on DMC calculations of the zero-point energies of the dimer and isolated hydrogen and water. Further examination of the vibrational ground state wavefunction obtained from DMC simulations indicates that the hydrogen and water monomers undergo nearly free internal rotation, which agrees with earlier observations. For the trimer, the PES also reproduces dissociation energy and harmonic frequencies quite accurately. Harmonic-frequency analysis also shows that the three-body interaction is not negligible for an accurate estimate of the harmonic frequency of the $H_2$ stretch. Finally, the PES has been applied to the $H_2@(H_2O)_{20}$ cluster for calculation of its dissociation energy. The contribution of the total $H_2-H_2O$ two-body and $H_2-H_2O-H_2O$ three-body interaction in this $H_2@(H_2O)_{20}$ cluster agrees very well with *ab initio* calculations, thus demonstrating the reliability of the PES in describing the $H_2$ clathrate hydrate.

Future development may include the evaluation of three-body contributions to translation-rotation energy levels, $H_2$ vibration and cage occupancy in $H_2$ clathrate hydrates. Construction of $H_2-H_2$ two-body, $(H_2)_3$ three-body and $H_2-H_2-H_2O$ three-body potentials will permit to build a PES capable of describing $(H_2)_m(H_2O)_n$ clusters, with the aim to investigate hydrogen storage capability and other properties of hydrogen clathrate hydrates.

PESs are available upon request.

## ACKNOWLEDGMENTS

J.M.B. thanks Alexandre Faure for sending code to evaluate the $H_2-H_2O$ potential in Ref. 9. as this manuscript was being written. Z. H. and C. Q. acknowledge the Army Research Office ARO-W911NF-14-1-0208 for financial support, R. C. acknowledges the U.S. Department of Energy, Office of Science, Office of Basic Energy Sciences, Award Number DE-

FG02-97ER14782 for financial support, and J.M.B. acknowledges both grants for financial support.

## REFERENCES


[1]Q. Zhang, Y. Ma, F. Fish, M. M. Szczęsńiak, and V. Buch, J. Chem. Phys. **96**, 6039 (1992).

[2]M. J. Weida and D. J. Nesbitt, J. Chem. Phys. **110**, 156 (1999).

[3]X.-G. Wang and T. Carrington, J. Chem. Phys. **134**, 044313 (2011).

[4]T. Zeng, H. Li, R. J. Le Roy, and P.-N. Roy, J. Chem. Phys. **135**, 094394 (2011).

[5]A. van der Avoird and D. J. Nesbitt, J. Chem. Phys. **134**, 044314 (2011).

[6]M. P. Ziemkiewicz, C. Pluetzer, D. J. Nesbitt, Y. Scribano, A. Faure, and A. van der Avoird, J. Chem. Phys. **137**, 084301 (2012).

[7]M. P. Hodges, R. J. Wheatley, G. K. Schenter, and A. H. Harvey, J. Chem. Phys. **120**, 710 (2004).

[8]A. Faure, P. Valiron, M. Wernli, L. Wiesenfeld, C. Rist, J. Noga, and J. Tennyson, J. Chem. Phys. **122**, 221102 (2005).

[9]P. Valiron, M. Wernli, A. Faure, L. Wiesenfeld, C. Rist, S. Kedžuch, and J. Noga, J. Chem. Phys. **129**, 134306 (2008).

[10]E. D. Sloan and C. A. Koh, *Clathrate hydrates of natural gases* (CRC Press, Taylor & Francis Group, 2008) pp. 1–44.

[11]J. A. Ripmeester, J. S. Tse, C. I. Ratcliffe, and B. M. Powell, Nature **325**, 135 (1987).

[12]W. L. Mao, H.-K. Mao, A. F. Goncharov, V. V. Struzhkin, Q. Guo, J. Hu, J. Shu, R. J. Hemley, M. Somayazulu, and Y. Zhao, Science **297**, 2247 (2002).

[13]W. L. Mao and H.-K. Mao, Proc. Natl. Acad. Sci. USA **101**, 708 (2004).

[14]L. J. Florusse, C. J. Peters, J. Schoonman, K. C. Hester, C. A. Koh, S. F. Dec, K. N. Marsh, and E. D. Sloan, Science **306**, 469 (2004).

[15]H. Lee, J. Lee, D. Y. Kim, J. Park, Y.-T. Seo, H. Zeng, I. L. Moudrakovski, C. I. Ratcliffe, and J. A. Ripmeester, Nature **434**, 743 (2005).

[16]F. Takeuchi, M. Hiratsuka, R. Ohmura, S. Alavi, A. K. Sum, and K. Yasuoka, J. Chem. Phys. **138**, 124504 (2013).

[17]S. Patchkovskii and J. S. Tse, Proc. Natl. Acad. Sci. USA **100**, 14645 (2003).

[18]P. K. Chattaraj, S. Bandaru, and S. Mondal, J. Phys. Chem. A **115**, 187 (2011).

[19]T. A. Strobel, C. J. Taylor, K. C. Hester, S. F. Dec, C. A. Koh, K. T. Miller, and E. D. Sloan, J. Phys. Chem. B **110**, 17121 (2006).

[20]R. Anderson, A. Chapoy, and B. Tohidi, Langmuir **23**, 3440 (2007).

[21]Á. Martín and C. J. Peters, J. Phys. Chem. B **113**, 7558 (2009).

[22]S. Alavi, J. A. Ripmeester, and D. D. Klug, J. Chem. Phys. **123**, 024507 (2005).

[23]N. I. Papadimitriou, I. N. Tsimpanogiannis, A. T. Papaioannou, and A. K. Stubos, J. Phys. Chem. B **112**, 10294 (2008).

[24]F. Sebastianelli, M. Xu, and Z. Bačić, J. Chem. Phys. **129**, 244706 (2008).

[25]F. Sebastianelli, M. Xu, Y. S. Elmatad, J. W. Moskowitz, and Z. Bačić, J. Phys. Chem. C **111**, 2497 (2007).

[26]Á. Valdés and G.-J. Kroes, J. Phys. Chem. C **116**, 21664 (2012).

[27]P. M. Felker, J. Chem. Phys. **138**, 174306 (2013).

[28]D.-Y. Koh, H. Kang, J. Jeon, Y.-H. Ahn, Y. Park, H. Kim, and H. Lee, J. Phys. Chem. C **118**, 3324 (2014).

[29]S. Alavi and J. A. Ripmeester, Angew. Chem. Int. Ed. **46**, 6102 (2007).

[30]T. T. Trinh, M. H. Waage, T. S. van Erp, and S. Kjelstrup, Phys. Chem. Chem. Phys. **17**, 13808 (2015).

[31]M. Xu, Y. S. Elmatad, F. Sebastianelli, J. W. Moskowitz, and Z. Bačić, J. Phys. Chem.

B **110**, 24806 (2006).

[32]A. Witt, F. Sebastianelli, M. E. Tuckerman, and Z. Bačić, J. Phys. Chem. C **114**, 20775 (2010).

[33]Á. Valdés and G.-J. Kroes, Phys. Chem. Chem. Phys. **13**, 2935 (2011).

[34]M. Xu, F. Sebastianelli, and Z. Bačić, J. Chem. Phys. **128**, 244715 (2008).

[35]D. Colognesi, M. Celli, L. Ulivi, M. Xu, and Z. Bačić, J. Phys. Chem. A **117**, 7314 (2013).

[36]H.-J. Werner, P. J. Knowles, G. Knizia, F. R. Manby, M. Schütz, P. Celani, T. Korona, R. Lindh, A. Mitrushenkov, G. Rauhut, K. R. Shamasundar, T. B. Adler, R. D. Amos, A. Bernhardsson, A. Berning, D. L. Cooper, M. J. O. Deegan, A. J. Dobbyn, F. Eckert, E. Goll, C. Hampel, A. Hesselmann, G. Hetzer, T. Hrenar, G. Jansen, C. Köppl, Y. Liu, A. W. Lloyd, R. A. Mata, A. J. May, S. J. McNicholas, W. Meyer, M. E. Mura, A. Nicklass, D. P. O'Neill, P. Palmieri, D. Peng, K. Pflüger, R. Pitzer, M. Reiher, T. Shiozaki, H. Stoll, A. J. Stone, R. Tarroni, T. Thorsteinsson, M. Wang, and A. Wolf, "Molpro, version 2010.1, a package of ab initio programs," (2010), see http://www.molpro.net.

[37]C. Qu, R. Conte, P. L. Houston, and J. M. Bowman, Phys. Chem. Chem. Phys. **17**, 8172 (2015).

[38]R. Conte, C. Qu, and J. M. Bowman, J. Chem. Theory Comp. **11**, 1631 (2015).

[39]V. Babin, G. R. Medders, and F. Paesani, Journal of Chemical Theory and Computation **10**, 1599 (2014), http://dx.doi.org/10.1021/ct500079y.

[40]B. J. Braams and J. M. Bowman, Int. Rev. Phys. Chem. **28**, 577 (2009).

[41]Z. Xie and J. M. Bowman, J. Chem. Theory Comp. **6**, 26 (2010).

[42]R. Conte, P. L. Houston, and J. M. Bowman, J. Chem. Phys. **140**, 151101 (2014).

[43]A. B. McCoy, Int. Rev. Phys. Chem. **25**, 77 (2006).

[44]J. B. Anderson, J. Chem. Phys. **63**, 1499 (1975).

[45]J. B. Anderson, J. Chem. Phys. **65**, 4121 (1976).

[46]I. Kosztin, B. Faber, and K. Schulten, Am. J. Phys. **64**, 633 (1996).

[47]D. W. Schwenke, J. Chem. Phys. **89**, 2076 (1988).

[48]H. Partridge and D. W. Schwenke, J. Chem. Phys. **106**, 4618 (1997).

[49]J. M. Bowman, S. Carter, and X. Huang, Int. Rev. Phys. Chem. **22**, 533 (2003).

[50]Y. Wang, X. Huang, B. C. Shepler, B. J. Braams, and J. M. Bowman, J. Chem. Phys. **134**, 094509 (2011).